Applied and Computational Mechanics 10 (2016) 97–110

Applied and Computational Mechanics

Influence of mesh density on calculated extreme stresses in aortic aneurysms

V. Man[a], S. Polzer[a], J. Burša[a,*]

[a] *Institute of Solid Mechanics, Mechatronics and Biomechanics, Brno University of Technology, Technická 2896/2, 616 69 Czech Republic*

Received 11 October 2016; received in revised form 10 December 2016

Abstract

The paper deals with evaluation of the influence of finite element mesh density on the resulting extreme stresses in models of abdominal aortic aneurysms. In most patient-specific computational models published recently, a free mesh of tetrahedrons is used and any information on density of the applied mesh is often missing. In this study a comparison of different mesh densities has been realized with four patient-specific model geometries, all based on a numerical reconstruction of the unloaded geometry of the aneurysm, and with two different Yeoh-type constitutive models. It has been shown that resulting maximum stresses are not mesh independent; due to a better description of the stress gradient in the critical location, the maximum wall stress increases with increasing number of elements throughout the wall thickness, especially in models without residual stresses. This effect is more pronounced when using Vande Geest constitutive model with higher strain stiffening than for Raghavan-Vorp material parameters. Although the mesh density requirements were not so high when the stress gradient was reduced by taking residual stresses into consideration, even in this case low numbers of elements throughout the wall thickness may give mesh dependent results. Although for a rigorous recommendation of the mesh density more analyses are needed, it was shown that the time consuming procedure of taking residual stresses into consideration cannot be replaced by a simpler model with rough mesh.

Keywords: abdominal aortic aneurysm, finite element model, peak wall stress, mesh density

1. Introduction

Abdominal aortic aneurysm (AAA) is defined as a dilatation of aortic diameter by more than 50 % against normal aorta [44]. In clinical practise, AAAs larger than 5.5 cm or growing by more than 0.5 cm/year [22, 23, 34] and [27] are assessed as severe and indicated for treatment, either to traditional open surgery or endovascular aneurysm repair (EVAR) [42]. Although in some trials EVAR has demonstrated an improved perioperative mortality and major morbidity when compared with the surgical open repair, some potential disadvantages exist — the risk of incomplete AAA sealing with subsequent development of continuous refilling of the aneurysm sac (depends on morphology of the AAA and pelvic arteries), increased radiation exposure during the treatment and the follow-up and, according to some studies (e.g. [26]), worse long-term results with more frequent re-interventions.

However, the major problem in AAA treatment is that even smaller AAAs may rupture and on the contrary, some AAAs grow up to 10 cm without rupture, when no treatment is applied. The above criterion of maximum diameter and growth speed is evidently not very reliable. It was shown [7, 20, 21] that computational models may give better prediction of rupture risk and help surgeons to avoid unnecessary surgeries. In last few years, finite element (FE) models based on

*Corresponding author. Tel.: +420 541 142 868, e-mail: bursa@fme.vutbr.cz.

real patient-specific AAA geometry have been widely applied in evaluation of peak wall stress (PWS) and peak wall rupture risk (PWRR) [6, 8, 10, 13, 24, 29, 39, 45, 49]. These quantities have been shown to predict the rupture risk better than the above geometrical criteria.

In creation of FE models, many authors use either shell elements [36], linear tetrahedral free mesh [19] with typically three or less elements across the wall, or hexahedral dominant mesh with one [1] or two [24, 39] elements throughout the wall thickness; in our group we use pure hexahedral mesh [30] with four elements across the wall. On the contrary, authors who analyse idealized geometries of AAAs use much finer meshes with some 4–10 elements across the wall [42,48]. Moreover, most of the authors do not specify how did they assess sufficiency of the mesh density [16,40,46]; sometimes they have only somehow increased the number of elements compared to the previous refinement step without an exact specification [41]. The reason is that rigorous approaches like reducing the element size to half or increasing the number of elements across the thickness would increase the number of elements dramatically; since isotropic meshes are mostly used in literature [19,43], it would become impossible for most computers to perform more than one such refinement. Unfortunately such refinement of a free mesh is done mostly along the surface and does not increase the number of elements in radial direction.

Clearly, the mesh density in the critical locations may be decisive for the accuracy of the resulting values and a too rough mesh can underestimate the extreme values substantially, especially in locations with high stress gradients. Therefore analysis of the required mesh density becomes necessary; to our best knowledge, however, there is no publication dealing with the impact of the number of elements throughout the wall thickness on the accuracy of the numerical results of AAA stress-strain analyses. Therefore we have decided to investigate this problem and to estimate how fine the mesh needs to be to provide stresses independent on its density.

2. Materials and methods

2.1. Geometry of AAA

The geometries of four AAAs ($n = 4$) were obtained from the CT-A scans of the aorta of patients indicated for elective repair at St. Anne's University Hospital, Brno, Czech Republic. We used commercial software (A4research vers. 3.0, VASCOPS GmbH, Austria) to reconstruct the 3D geometry and to acquire STL data of the wall and intraluminal thrombus (ILT). The approach applied by this software and its accuracy was described in [1, 18]. It is based on application of a virtual balloon to obtain a very accurate model of the inner surface of AAA without any artefacts which could induce non-realistic stress concentrations in the model; this is one of the reasons why stress gradients in tangential directions are relatively small and the mesh density is tested in radial direction only. The wall thickness is assumed to be constant (1.5 mm) because its value cannot be determined from the CT scans. The STL data were further processed in ICEM ver. 14.5 (ANSYS Inc., PA, USA) which allowed us to create a pure hexahedral mesh on the patient-specific geometries. This choice is motivated by the possibility of easy changing the number of elements (from two to six) in radial direction which does not affect the number of elements in other directions and thus the total number of elements increases only linearly during refinement. A pure hexahedral mesh, however, requires to be created manually with irregular geometries; creation of a mesh on a patient-specific AAA geometry took approximately 6 hours of operator's work. Till now, this approach has been applied only by our group [30]. In our models the linear hexahedral FEs were applied for the AAA wall, while the ILT was meshed by linear tetrahedral elements with element size of 3 mm (mixed formulation element of the type solid 285 according to ANSYS terminology, suitable for modelling of incompressible

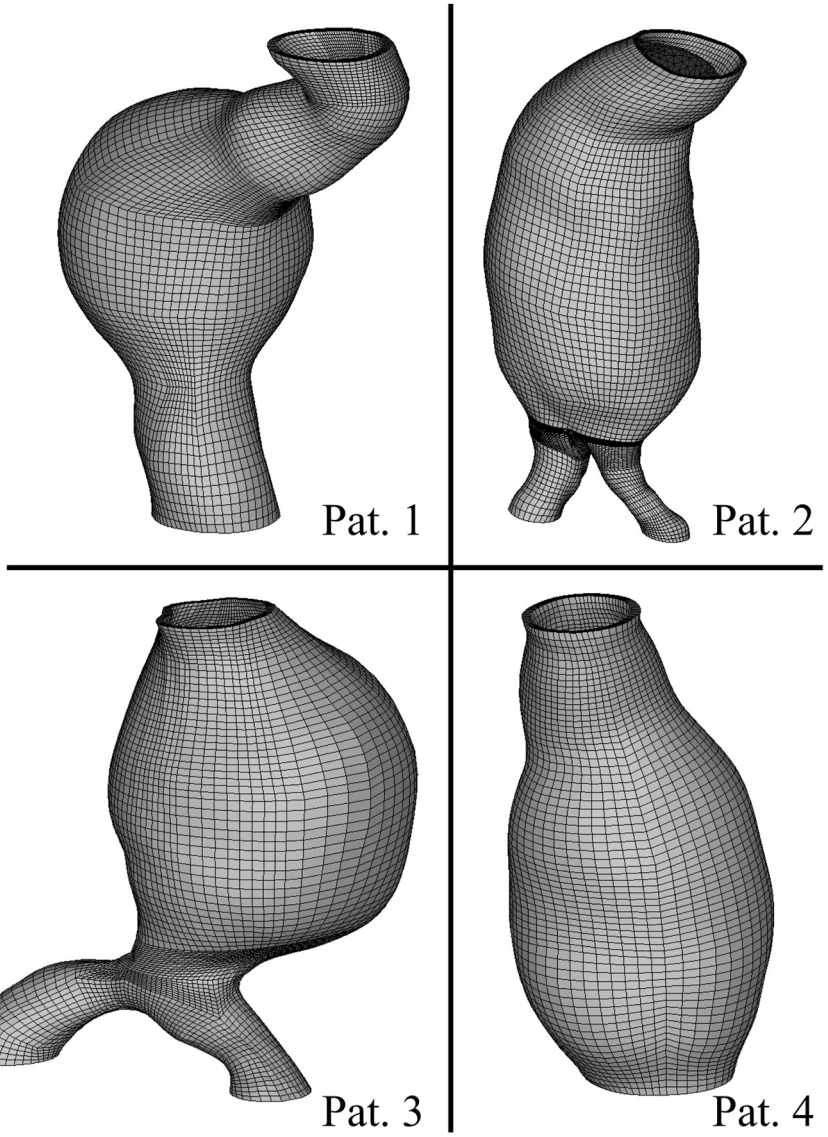

Fig. 1. FE meshes of the investigated AAAs. These meshes had following numbers of elements (when 2 elements across the wall were considered: Pat. 1. Wall-13.5k, ILT 29.7k; Pat. 2. Wall 18.5k, ILT 76k; Pat. 3. Wall 13.5k, ILT 31.6k; Pat. 4. Wall 7.6k, ILT 3.7k

materials [28]). Mesh convergence for ILT was not investigated although our previous analyses have shown that the results still slightly depend on the mesh with this element size. However, we evaluate stresses in the AAA wall only and the same ILT mesh was used for all gradually refined wall meshes thus it should not affect our conclusions. FE models of the investigated AAAs are shown in Fig. 1.

2.2. Constitutive models

2.2.1. AAA wall model

Mechanical properties of the wall reported in literature vary significantly [14, 37], and we have previously shown that the shape of the stress-strain curve heavily affects the stress distribution across the wall even for an ideal tube [31]. Therefore we have analysed two fundamentally different types of material models; similarly to [39], both of them are isotropic due to lack of information on distribution of directions of collagen fibres in AAA wall. The former is the so

called Raghavan Vorp model (RV) based on uniaxial tensile tests of AAA wall tissue [37] which applies a hyperelastic fully incompressible isotropic 2nd order Yeoh constitutive model with strain energy density function ψ formulated as follows:

$$\psi = \sum_{i=1}^{2} c_{i0}(I_1 - 3)^i. \tag{1}$$

Here c_{i0} represent stress-like material constants, I_1 is the first invariant of Cauchy-Green deformation tensor. For this model the parameters were specified as $c_{10} = 177$ kPa and $c_{20} = 1\,881$ kPa which reflect mean population data for AAAs [37].

The latter considered material model is the so called Vande Geest model (VG). Specifically, 5th order Yeoh model was applied with a similar strain energy density function [31]:

$$\psi = \sum_{i=1}^{5} c_{i0}(I_1 - 3)^i. \tag{2}$$

Specific material constants of this model were based on experiments by Vande Geest et al. [14]. However, they fitted the results of AAA tissue testing with the anisotropic constitutive model proposed by Choi and Vito [4] while we use an isotropic one in this study. Moreover, they have fitted the experimental curves separately for all of the 26 patients and then the average material parameters were obtained as average of all the calculated material parameters. As the same or very similar experimental results can be fitted with different sets of material parameters of the same constitutive model (this holds especially for phenomenological models), we consider this approach disputable. Therefore we carried out numerical simulations of all of the equibiaxial and proportional tensile tests of 26 patients with their patient-specific material parameters published in [14]; all these simulated tests together were then fitted with the above model (Eq. (2)), and the following set of constants was obtained: $c_{10} = 0.5$ kPa, $c_{20} = 0$ kPa, $c_{30} = 0$ kPa, $c_{40} = 2\,200$ kPa, $c_{50} = 13\,741$ kPa. Both constitutive models were applied in mixed formulation as fully incompressible, their comparison is shown in Fig. 2.

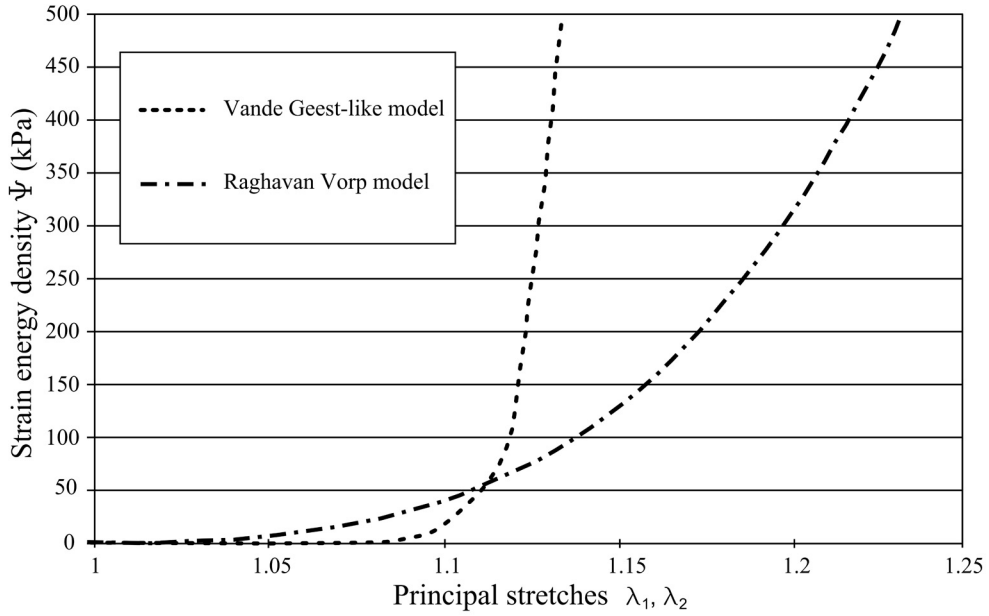

Fig. 2. Comparison of both applied strain energy density functions representing mean population data at equi-biaxial stretches of the abdominal aortic aneurysm (AAA) wall

2.2.2. ILT model

Despite its porous nature, ILT was modelled as a single phase isotropic hyperelastic fully incompressible (mixed formulation) material because it was previously shown this simplification does not affect wall stresses in AAA [32]. ILT exhibits nearly linear behaviour, which can be described by the following one-parameter Ogden-like strain energy function:

$$\psi = c\sum_{i=1}^{3}(\lambda_i^4 - 1), \tag{3}$$

where the material parameter c must be identified experimentally, and λ_i denotes the i-th principal stretch. According to [11] we used values of the material parameter varying throughout the ILT thickness, namely $c = 2.62$ kPa at the luminal side and $c = 1.73$ kPa at the abluminal side (or for areas more distant than 30 mm from the lumen).

2.3. Finite element analyses

It is well known that the geometries reconstructed from the CT scans describe in vivo (loaded) conditions while for FE analysis a stress-free geometry is required. Respecting of unloaded geometry is consistently shown as an important feature of FEA of AAAs [5]. Several methods for reconstruction of the unloaded geometry have been recently created [12, 30, 31, 41]; one of them is applied in our models [30]. Briefly, it is assumed that each AAA was loaded by the mean blood pressure of 13 kPa at the time of scanning. To find the unloaded geometry an iterative algorithm is applied where in the first iteration the original geometry is loaded by the mean blood pressure and the obtained displacements are then subtracted from the original geometry which generates a new reconstructed unloaded geometry. This geometry is then loaded by the same pressure and its deviation from the original geometry is evaluated. Then next iterations are performed unless the deviation is below a chosen limit or the maximum number of iterations is reached.

Each aneurysm with the reconstructed unloaded patient-specific geometry was constrained in all directions at the proximal and distal ends. A rigid contact was considered between the wall and ILT, the effect of the surrounding tissue was neglected. The blood pressure of 13 kPa was applied at the inner surface of the AAA wall.

Then the mesh sensitivity was tested by comparing PWS for meshes with various numbers of elements in radial direction. Due to possible stress singularities, the regions of AAA edges and bifurcation were excluded from the analyses. The PWS was extracted as von Mises stress of the nodal solution, i.e. average value from all the neighbouring elements of the respective node. In this way we have analysed two sets of FE models for each considered material model. First, only unloaded geometry was respected as described above. The second computational model assessed the mesh sensitivity when algorithm for incorporating residual stresses (RS) [29] was executed after having found the unloaded geometry. RS exist in arteries and they decrease stress gradients across the wall [9] thus it is expected their presence will also influence the required mesh size. We used volumetric growth method [29] which is currently the only approach which was verified to work with irregular AAA geometries.

We started the analyses with 2 elements across the AAA wall and then increased this number gradually. The acceptability of the results for a specific mesh density was assessed on the basis of percentual deviation of the von Mises PWS from the value obtained with the closest lower number of elements throughout the wall; if this deviation was less than 5 %, the mesh was assessed as acceptable and the increase of mesh density was not more continued.

Finally, some authors use radially rough mesh on purpose [10] to reduce stress gradients and thus avoid the necessity of using time consuming algorithms for RS. Therefore we have also compared PWS calculated in the roughest mesh models (with 2 elements across the wall thickness) without RS with those obtained in the models with RS and the finest mesh.

3. Results and discussion

All the analyses were carried out with PC 4 CPU, 12 GB RAM. As the computation of the unloaded geometry as well as the RS algorithm are iterative, requirements on computer time were rather high and computations took about 20 hours per case. For each patient up to 15 simulations were carried out, differing from each other not only by the number of elements but also by the constitutive model applied, and whether the residual stresses were taken into account or not.

3.1. Constitutive model RV

The unloaded geometry was found accurately enough in all cases. The maximum deviation from the original geometry was below 0.5 mm (less than CT resolution), in 90 % of nodes the deviation was less than 0.15 mm. An example of results is shown in Fig. 3. The outputs from the FEA using the RV material model are shown in Table 1 (for models without RS) and in Table 2

Table 1. Unloaded geometry without residual stresses, model Raghavan-Vorp. Maximum von Mises stresses (kPa) and their percentual deviations for the individual FE models of AAAs with varying mesh density

Patient no.		No. of elements			
		2	3	4	5
1	von Mises stress (kPa)	178	208	209	–
	percentual deviation (%)	–	17	0.3	–
2	von Mises stress (kPa)	179	194	202	–
	percentual deviation (%)	–	8.2	4.2	–
3	von Mises stress (kPa)	161	202	303	311
	percentual deviation (%)	–	25.6	49.5	2.9
4	von Mises stress (kPa)	246	287	295	–
	percentual deviation (%)	–	16.6	2.9	–

Table 2. Unloaded geometry with residual stresses, model Raghavan-Vorp. Maximum von Mises stresses (kPa) and their percentual deviations for the individual FE models of AAAs with varying mesh density

Patient no.		No. of elements			
		2	3	4	5
1	von Mises stress (kPa)	154	161	–	–
	percentual deviation (%)	–	4	–	–
2	von Mises stress (kPa)	137	138	–	–
	percentual deviation (%)	–	0.7	–	–
3	von Mises stress (kPa)	197	204	–	–
	percentual deviation (%)	–	3.5	–	–
4	von Mises stress (kPa)	168	214	170	165
	percentual deviation (%)	–	27	26	3

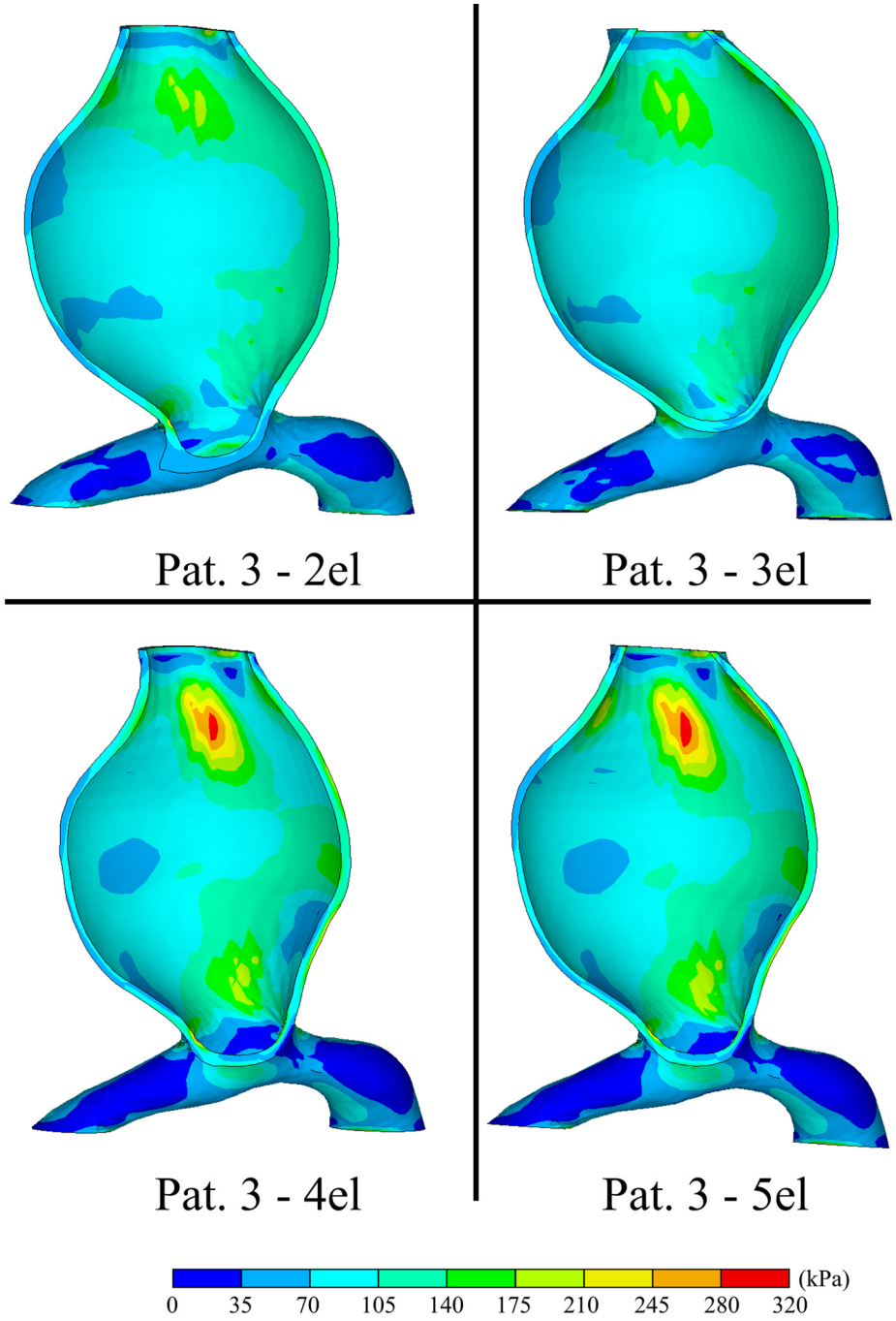

Fig. 3. Contour plots of the PWS stresses in the aneurysm wall for different numbers of elements throughout the wall thickness for patient 4, RV model, RS neglected. ILT is not shown

(for models with RS). It is noted that due to the influence of boundary conditions, the vicinity of both ends of AAAs was excluded from the analyses, as well as the region of bifurcation. Table 1 shows that 5 elements across the wall are needed to capture the stresses with the required accuracy in all cases.

3.2. Constitutive model VG

Results of the models without residual stresses are presented in Table 3. For this constitutive model the maximum number of 6 elements in transmural direction still was not sufficient to obtain an error below 5 % for three of the patients. When RS was included the mesh with 4 elements across the wall became sufficient in all cases, as shown in Table 4.

The comparison of rough mesh without RS and the finest mesh with RS gave deviations in PWS of 36 %, 71 %, 55 % and 103 % for the individual cases, respectively.

Table 3. Unloaded geometry without residual stresses, model Vande Geest. Maximum von Mises stresses (kPa) and their percentual deviations for the individual FE models of AAAs with varying mesh density

Patient no.		No. of elements				
		2	3	4	5	6
1	von Mises stress (kPa)	329	415	516	475	516
	percentual deviation (%)	–	26.3	24.3	7.9	8.7
2	von Mises stress (kPa)	200	244	276	300	319
	percentual deviation (%)	–	21.9	13.1	8.7	6.5
3	von Mises stress (kPa)	383	496	588	**633**	**669**
	percentual deviation (%)	–	29.5	18.5	7.7	5.7
4	von Mises stress (kPa)	426	508	581	**638**	**682**
	percentual deviation (%)	–	19.4	14.4	9.6	7

Table 4. Unloaded geometry with residual stresses, model Vande Geest. Maximum von Mises stresses (kPa) and their percentual deviations for the individual FE models of AAAs with varying mesh density

Patient no.		No. of elements			
		2	3	4	5
1	von Mises stress (kPa)	176	205	232	242
	percentual deviation (%)	–	16.4	13.2	4.3
2	von Mises stress (kPa)	116	117	–	–
	percentual deviation (%)	–	0.9	–	–
3	von Mises stress (kPa)	204	240	247	–
	percentual deviation (%)		17.6	2.9	–
4	von Mises stress (kPa)	184	202	210	–
	percentual deviation (%)	–	9.8	4	–

3.3. Discussion

FEA represents a hopeful approach in assessment of the patient-specific PWS eventually PWRR. To assess the accuracy of the results, the authors of this study used FE models with increasing number of elements throughout the wall thickness, and the impact of this number of elements on the calculated extreme stresses was evaluated. When using RV model the necessary number of elements across the wall thickness was between 3 and 5 to obtain the stresses independent of the mesh. This is a surprisingly high number since most studies analysing real AAAs do not use such a fine mesh [24, 39]. On the other hand it justifies the mesh choice in studies where idealized geometries were analysed [42, 48] and highlights the need of using finer meshes in FEA of patient specific geometries of AAA.

The situation is even worse when VG model is used because omitting of RS may cause that more than 6 elements in radial direction are required to capture the wall stress with sufficient accuracy. We did not further increase the number of elements in radial direction because we experienced convergence problems due to worse and worse aspect ratio of the finite elements which made them inclinable to excessive distortion during deformation. This could be solved by complete recreation of the mesh which would be, however, too time consuming. Moreover we are not aware of any study where 6 elements across the wall would be used for patient-specific geometries, thus our results are sufficient to show unacceptability of such models. Based on our results we can hypothesize the mesh independent results could be obtained for 7 radial elements. This information is however not that important since the importance of RS is widely accepted nowadays [2, 3, 17, 35]. Without taking them into consideration the calculated stresses may even exceed the strength of the AAA tissues (cf. [50] and [42]). Also for some patients in our study the stresses calculated with neglecting residual stresses (see Table 3 do exceed the strength values of AAA tissue which corresponds to 600 ± 150 kPa according to [50]. As all the patients were CT-scanned without any symptoms of rupture, it is evident that the calculated stress values exceeding the tissue strength are incorrect. On the contrary, results taking RS into consideration show much lower PWS and suggest (see Table 4) that four elements across the wall should be sufficient in most cases which retroactively validates the meshes we used previously [30].

Another interesting result of our analysis reveals that we cannot confirm the hypothesis adopted by some authors [10, 30] stating it is possible to omit RS and still obtain accurate stresses when using rough mesh with only one or two elements across the wall. We have clearly shown that difference between both approaches for RV and VG model can be up to 49 % and 103 %, respectively. Although this was obtained on a cohort of patients being very small for verification of the hypothesis, its size is sufficient for its falsification when the deviation is as large in most cases; including more patients would likely reveal even larger differences. This hypothesis can be rejected on the basis of the presented results and use of RS algorithm together with a sufficiently fine mesh is recommended instead.

Our results have also shown that a rougher mesh is sufficient when residual stresses are included compared to the model without RS. This conclusion is in accordance with our expectations based on substantial reduction of stress gradients by considering RS and reduce spatially the increase of computational time due to inclusion of the RS algorithm.

Any results must be viewed with respect to their limitations. One limitation of this study is absence of patient-specific values of blood pressure. The reconstructed geometry depends on the actual blood pressure under which the CT scans were recorded which, moreover, changes slightly with location in the arterial tree [25]. For hypertensive patients this value may be influenced by the

foregoing (e.g. antihypertensive) medication having been applied to decelerate the AAA growth. Of course, the patient-specific blood pressure is crucial when AAA rupture risk assessment is performed [10, 30]. Nevertheless, our approach using the same mean population value of blood pressure is fully applicable for comparison of results with different mesh densities although the stresses might be slightly different even for the models with RS if patient-specific pressure was applied.

The very low cohort of investigated geometries represents another limitation. This was caused by large number of FEA performed on each AAA (52 FEAs in total) which makes the computations very time consuming. However, even within this small number of patients there were analyses in which low numbers of elements across the wall thickness gave severe deviations in resulting stresses. Consequently analyses with low numbers of elements across the wall thickness lose their credibility. Naturally, for a quantitative recommendation for mesh density more analyses are needed.

Another limitation is in applying isotropic approximation of VG constitutive models. However we do not consider this as a severe limitation because inter-patient variability of aneurysmal wall mechanical properties is much higher than the reported level of its anisotropy [18]. It was also shown that anisotropy of AAA wall is much lower than that of healthy aortic wall [14], that interpatient variability is much higher than inter-direction variability due to anisotropy [38, 39, 47], and that differences based on application of anisotropic model are statistically insignificant [15]. Thus the mean population response can be captured by isotropic or anisotropic models with a similar accuracy. Moreover, for correct application of anisotropic models it is necessary to know the local orientation of principal material directions in the AAA wall which is currently unknown and quite not easy to be defined for complex shapes of AAAs.

Also tetrahedral mesh for the ILT and its density might be disputable; however, creation of a hexahedral mesh also for the ILT is even much more difficult (if even possible) than it was for the AAA wall. The stresses in the ILT are not evaluated in this study and their accuracy cannot influence the PWS substantially [33]. Moreover, the individual models of each patient had always the same ILT mesh therefore its impact on the wall stress is the same. Consequently, it cannot alter the conclusions drafted here on the basis of comparing the models. Moreover, a further refinement of the ILT mesh would cause that the data for FEA would not fit to RAM memory of our PC which would increase computational time several times. That is why we used 3 mm elements in the ILT mesh.

4. Conclusions

The presented analyses confirmed that the influence of mesh density is substantial in FE modelling of AAAs although their geometry meets the conditions of membrane shells with nearly constant stresses throughout the wall thickness. The higher is the strain stiffening of the material, the higher are the stress gradients across the wall and consequently the impact of mesh density on the resulting stresses in the models neglecting residual stresses. For some of these models no mesh independent results were obtained in the investigated range of mesh densities despite we used finer mesh than any previous study investigating patient specific geometries of AAA. This highlights the necessity of using even finer mesh when substantial stress gradients across the wall should be captured.

For the models comprehending RS, the stress gradients across the wall are much lower. Consequently the influence of mesh density was less pronounced and a reasonable number of elements across the AAA wall (5 or less) was sufficient to capture the PWS with acceptable

accuracy in all of the investigated cases. However, for a general quantitative recommendation of this number of elements a larger study is needed.

By comparison of the results it was clearly shown that the time consuming procedure of reducing stress gradients across the wall thickness by taking RS into consideration cannot be replaced by a much faster model with a rough mesh and without RS. Although both of these approaches may give similarly low stress gradients across the wall, the simple model with rough mesh without RS cannot give correct values of peak wall stresses.

Acknowledgements

This work is an output of project NETME CENTRE PLUS (LO1202), created with financial support from the Ministry of Education, Youth and Sports under the National Sustainability Programme I.

References

[1] Auer, M., Gasser, T., Reconstruction and finite element mesh generation of abdominal aortic aneurysms from computerized tomography angiography data with minimal user interactions, IEEE Transactions on Medical Imaging 29 (4) (2010) 1022–1028.

[2] Balzani, D., Schröder, J., Gross, D., Numerical simulation of residual stresses in arterial walls, Computational Materials Science 39 (1) (2007) 117–123.

[3] Chaudhry, H., Bukiet, B., Davis, A., Ritter, A., Findley, T., Residual stresses in oscillating thoracic arteries reduce circumferential stresses and stress gradients, Journal of Biomechanics 30 (1) (1997) 57–62.

[4] Choi, H., Vito, R., Two-dimensional stress-strain relationship for canine pericardium, Journal of Biomechanical Engineering 112 (2) (1990) 153–165.

[5] de Putter, S., Wolters, B., Rutten, M., Breeuwer, M., Gerritsen, F., van de Vosse, F., Patient-specific initial wall stress in abdominal aortic aneurysms with a backward incremental method, Journal of Biomechanics 40 (5) (2007) 1081–1090.

[6] Doyle, B., Coyle, P., Kavanagh, E., Grace, P., McGloughlin, T., A finite element analysis rupture index (FEARI) assessment of electively repaired and symptomatic/ruptured abdominal aortic aneurysms, Journal of Vascular Surgery 31 (4) (2000) 883–886.

[7] Fillinger, M., Marra, S., Raghavan, M., Kennedy, F., Prediction of rupture risk in abdominal aortic aneurysm during observation: Wall stress versus diameter, Journal of Vascular Surgery 37 (4) (2003) 724–732.

[8] Fillinger, M., Raghavan, M., Marra, S., Cronenwett, J., Kennedy, F., Kuhan, G., Chetter, I., McCollum, P., In vivo analysis of mechanical wall stress and abdominal aortic aneurysm rupture risk, Journal of Vascular Surgery 36 (3) (2002) 589–597.

[9] Fung, Y. C., Biomechanics – Mechanical properties of living tissues, Springer-Verlag, 1993.

[10] Gasser, T. C., Auer, M., Labruto, F., Swedenborg, J., Roy, J., Biomechanical rupture risk assessment of abdominal aortic aneurysms: Model complexity versus predictability of finite element simulations, European Journal of Vascular and Endovascular Surgery 40 (2) (2010) 176–185.

[11] Gasser, T. C., Görgülü, G., Folkesson, M., Swedenborg, J., Failure properties of intraluminal thrombus in abdominal aortic aneurysm under static and pulsating mechanical loads, Journal of Vascular Surgery 48 (1) (2008) 179–188.

[12] Gee, M., Reeps, C., Eckstein, H., Wall, W., Buth, J., Breeuwer, M., Jacobs, M., van de Vosse, F., Prestressing in finite deformation abdominal aortic aneurysm simulation, Journal of Biomechanics 42 (11) (2009) 1732–1739.

[13] Geest, J. P. V., Di Martino, E., Bohra, A., Makaroun, M., Vorp, D. A., A biomechanics-based rupture potential index for abdominal aortic aneurysm risk assessment: Demonstrative application, Annals of the New York Academy of Sciences 1085 (1) (2006) 11–21.

[14] Geest, J. P. V., Sacks, M., Vorp, D. A., The effects of aneurysm on the biaxial mechanical behavior of human abdominal aorta, Journal of Biomechanics 39 (7) (2006) 1324–1334.

[15] Geest, J. P. V., Schmidt, D. E., Sacks, M. S., Vorp, D. A., The effects of anisotropy on the stress analyses of patient-specific abdominal aortic aneurysms, Annals of Biomedical Engineering 36 (6) (2008) 921–932.

[16] Heng, M., Fagan, M., Collier, J., Desai, G., McCollum, P., Chetter, I., Peak wall stress measurement in elective and acute abdominal aortic aneurysms, Journal of Vascular Surgery 47 (1) (2008) 17–22.

[17] Holzapfel, G., Sommer, G., Auer, M., Regitnig, P., Ogden, R., Layer-specific 3D residual deformations of human aortas with non-atherosclerotic intimal thickening, Annals of Biomedical Engineering 35 (4) (2007) 530–545.

[18] Hyhlik-Dürr, A., Krieger, T., Geisbüsch, P., Kotelis, D., Able, T., Böckler, D., Reproducibility of deriving parameters of AAA rupture risk from patient-specific 3D finite element models, Journal of Endovascular Therapy 18 (3) (2011) 289–298.

[19] Joldes, G. R., Miller, K., Wittek, A., Doyle, B., A simple, effective and clinically applicable method to compute abdominal aortic aneurysm wall stress, Journal of the Mechanical Behavior of Biomedical Materials 58 (2016) 139–148.

[20] Khosla, S., Morris, D. R., Moxon, J. V., Walker, P. J., Gasser, T. C., Golledge, J., Meta-analysis of peak wall stress in ruptured, symptomatic and intact abdominal aortic aneurysms, British Journal of Surgery 101 (11) (2014) 1350–1357.

[21] Kleinstreuer, C., Li, Z., Analysis and computer program for rupture-risk prediction of abdominal aortic aneurysms, BioMedical Engineering OnLine 5 (1) (2006) 19–32.

[22] Lederle, F., Wilson, S., Johnson, G., Reinke, D., Littooy, F., Acher, C., Ballard, D., Messina, L., Gordon, I., Chute, E., Krupski, W., Busuttil, S., Barone, G., Sparks, S., Graham, L., Rapp, J., Makaroun, M., Moneta, G., Cambria, R., Makhoul, R., Eton, D., Ansel, H., Freischlag, J., Bandyk, D., Immediate repair compared with surveillance of small abdominal aortic aneurysms, New England Journal of Medicine 346 (19) (2002) 1437–1444.

[23] Lederle, F., The aneurysm detection and management study screening program validation cohort and final results, Archives of Internal Medicine 160 (10) (2000) 1425–1430.

[24] Maier, A., Gee, M., Reeps, C., Pongratz, J., Eckstein, H., Wall, W., A comparison of diameter, wall stress, and rupture potential index for abdominal aortic aneurysm rupture risk prediction, Annals of Biomedical Engineering 38 (10) (2010) 3124–3134.

[25] Matthys, K., Alastruey, J., Peiró, J., Khir, A., Segers, P., Verdonck, P., Parker, K., Sherwin, S., Pulse wave propagation in a model human arterial network: Assessment of 1-D numerical simulations against in vitro measurements, Journal of Biomechanics 40 (15) (2007) 3476–3486.

[26] Moll, F., Powell, J., Fraedrich, G., Verzini, F., Haulon, S., Waltham, M., Van Herwaarden, J., Holt, P., van Keulen, J., Rantner, B., Schlösser, F., Setacci, F., Ricco, J., Management of abdominal aortic aneurysms clinical practice guidelines of the European Society for Vascular Surgery, European Journal of Vascular and Endovascular Surgery 41 (2011) S1–S58.

[27] Nicholls, S., Gardner, J., Meissner, M., Johansen, K., Rupture in small abdominal aortic aneurysms, Journal of Vascular Surgery 28 (5) (1998) 884–888.

[28] Oñate, E., Rojek, J., Taylor, R., Zienkiewicz, O., Finite calculus formulation for incompressible solids using linear triangles and tetrahedra, International Journal for Numerical Methods in Engineering 59 (11) (2004) 1473–1500.

[29] Polzer, S., Bursa, J., Gasser, T. C., Staffa, R., Vlachovsky, R., A numerical implementation to predict residual strains from the homogeneous stress hypothesis with application to abdominal aortic aneurysms, Annals of Biomedical Engineering 41 (7) (2013) 1516–1527.

[30] Polzer, S., Gasser, T. C., Biomechanical rupture risk assessment of abdominal aortic aneurysms based on a novel probabilistic rupture risk index, Journal of The Royal Society Interface 12 (113) (2015) No. 20150852, doi: 10.1098/rsif.2015.0852.

[31] Polzer, S., Gasser, T. C., Bursa, J., Staffa, R., Vlachovsky, R., Man, V., Skacel, P., Importance of material model in wall stress prediction in abdominal aortic aneurysms, Medical Engineering 35 (9) (2013) 1282–1289.

[32] Polzer, S., Gasser, T. C., Markert, B., Bursa, J., Skacel, P., Impact of poroelasticity of intraluminal thrombus on wall stress of abdominal aortic aneurysms, BioMedical Engineering OnLine 11 (1) (2012) 62–75.

[33] Polzer, S., Gasser, T., Swedenborg, J., Bursa, J., The impact of intraluminal thrombus failure on the mechanical stress in the wall of abdominal aortic aneurysms: Identification of a finite strain constitutive model and evaluation of its applicability. European Journal of Vascular and Endovascular Surgery 41 (4) (2011) 467–473.

[34] Powell, J. T., Brady, A. R., Brown, L. C., Forbes, J. F., Fowkes, F. G. R., Greenhalgh, R. M., Ruckley, C. V., Thompson, S. G., and UK Small Aneurysm Trial Participants, Mortality results for randomised controlled trial of early elective surgery or ultrasonographic surveillance for small abdominal aortic aneurysms, Lancet 352 (9141) (1998) 1649–1655.

[35] Raghavan, M., Trivedi, S., Nagaraj, A., McPherson, D., Chandran, K., Three-dimensional finite element analysis of residual stress in arteries, Annals of Biomedical Engineering, 32 (2) (2004) 257–263.

[36] Raghavan, M., Vorp, D., Federle, M., Makaroun, M., Webster, M., Wall stress distribution on three-dimensionally reconstructed models of human abdominal aortic aneurysm, Journal of Vascular Surgery 31 (4) (2000) 760–769.

[37] Raghavan, M., Vorp, D., Toward a biomechanical tool to evaluate rupture potential of abdominal aortic aneurysm: Identification of a finite strain constitutive model and evaluation of its applicability, Journal of Biomechanics 33 (4) (2000) 475–482.

[38] Reeps, C., Maier, A., Pelisek, J., Härtl, F., Grabher-Meier, V., Wall, W. A., Essler, M., Eckstein, H.-H., Gee, M. W., Measuring and modeling patient-specific distributions of material properties in abdominal aortic aneurysm wall, Biomechanics and Modeling in Mechanobiology 12 (4) (2013) 717–733.

[39] Reeps, C., Gee, M., Maier, A., Gurdan, M., Eckstein, H., Wall, W., The impact of model assumptions on results of computational mechanics in abdominal aortic aneurysm, Journal of Vascular Surgery 51 (3) (2010) 679–688.

[40] Rissland, P., Alemu, Y., Einav, S., Ricotta, J., Bluestein, D., Abdominal aortic aneurysm risk of rupture: Patient-specific FSI simulations using anisotropic model, Journal of Biomechanical Engineering 131 (3) (2009) No. 031001, doi: 10.1115/1.3005200.

[41] Riveros, F., Martufi, G., Gasser, T. C., Rodriguez, J. F., Influence of intraluminal thrombus topology on AAA passive mechanics, Proceedings of the 40th Annual Meeting on Computing in Cardiology (CinC), Zaragoza, IEEE, 2013, pp. 899–902.

[42] Rodríguez, J., Ruiz, C., Doblareé, M., Holzapfel, G., Mechanical stresses in abdominal aortic aneurysms: Influence of diameter, asymmetry, and material anisotropy, Journal of Biomechanical Engineering 130 (2) (2008) No. 021023, doi: 10.1115/1.2898830.

[43] Rodríguez, J. F., Martufi, G., Doblaré, M., Finol, E. A., The effect of material model formulation in the stress analysis of abdominal aortic aneurysms, Annals of Biomedical Engineering 37 (11) (2009) 2218–21.

[44] Sakalihasan, N., Limet, R., Defawe, O., Abdominal aortic aneurysm, Lancet 365 (9470) (2005) 1577–1589.

[45] Speelman, L., Bosboom, E., Schurink, G., Hellenthal, F., Buth, J., Breeuwer, M., Jacobs, M., van de Vosse, F., Patient-specific AAA wall stress analysis: 99-percentile versus peak stress, European Journal of Vascular and Endovascular Surgery 36 (6) (2008) 668–676.

[46] Speelman, L., Schurink, G., Bosboom, E., Buth, J., Breeuwer, M., van de Vosse, F., Jacobs, M., The mechanical role of thrombus on the growth rate of an abdominal aortic aneurysm, Journal of Vascular Surgery 51 (1) (2010) 19–26.

[47] Tong, J., Cohnert, T., Regitnig, P., Holzapfel, G. A., Effects of age on the elastic properties of the intraluminal thrombus and the thrombus-covered wall in abdominal aortic aneurysms: Biaxial extension behaviour and material modelling, European Journal of Vascular and Endovascular Surgery 42 (2) (2011) 207–219.

[48] Toungara, M., Chagnon, G., Geindreau, C., Numerical analysis of the wall stress in abdominal aortic aneurysm: Influence of the material model near-incompressibility, Journal of Mechanics in Medicine and Biology 12 (1) (2012) No. 1250005, doi: 10.1142/S0219519412004442.

[49] Venkatasubramaniam, A., Fagan, M., Mehta, T., Mylankal, K., Ray, B., Kuhan, G., Chetter, I., McCollum, P., A comparative study of aortic wall stress using finite element analysis for ruptured and non-ruptured abdominal aortic aneurysms, European Journal of Vascular and Endovascular Surgery 28 (2) (2004) 168–176.

[50] Vorp, D., Raghavan, M., Muluk, S., Makaroun, M., Steed, D., Shapiro, R., Webster, M., Wall strength and stiffness of aneurysmal and nonaneurysmal abdominal aorta, Annals of the New York Academy of Sciences 800 (1996) 274–276.